

# Development of a Wireless Pressure Measurement System Using Interdigitated Capacitors

Khalil I. Arshak, *Member, IEEE*, Deirdre Morris, Arousian Arshak, Olga Korostynska, and Essa Jafer

**Abstract**—Remote pressure monitoring is of particular importance in medical and environmental applications as it is less labour intensive, safer and offers peace of mind to the general public. To meet this demand, a prototype system has been developed and used to evaluate thick-film pressure sensors with an oxide dielectric layer. The circuit is based on the principle of capacitance-frequency-voltage conversion and has been designed to minimize power consumption. Each device was tested under hydrostatic pressure in the range 0–17 kPa and assessed in terms of sensitivity, hysteresis, repeatability, creep and temperature effects. The results show that this approach may be used for the fabrication of cost effective, reliable devices for wireless pressure sensing applications.

**Index Terms**—Dielectric materials, pressure measurement, telemetry, thick-film capacitors.

## I. INTRODUCTION

THERE is a significant need for continuous monitoring of environmental, industrial, and biological situations. In healthcare, aging populations and increased stress levels due to the modern pace of life mean that many hospitals and general practitioner's offices are under increasing pressure to meet the needs of their patients [1]. An ability to monitor people in their homes may result in a higher quality of life for patients, while creating more space in hospitals for emergencies and the critically ill. Of the various parameters of interest when monitoring a person's wellbeing, long-term pressure measurement is one of the most valuable for gaining further insight into physiological processes in the area of cardiology, gastroenterology, urology, neurology, and rehabilitation [2]. In the automotive industry, knowledge of tire temperature and pressure is essential, as a change in pressure can cause a reduction in driving stability, fuel consumption, tire life, and, in extreme cases, it is possible that it will burst, resulting in serious accidents [3], [4]. Also, aerodynamic pressure measurements are required for the safe

and effective design of aircraft, which is essential as passenger numbers continue to increase [5].

In designing a pressure monitoring system, requirements such as power consumption, device size, shape, reliability, and cost must be carefully considered [6]. They become particularly stringent when the system is to be used for biomedical monitoring as space and power is at a premium. With these considerations in mind, devices where pressure measurements are made by recording the variation in capacitance are preferred. They are suited to wireless systems due to their high sensitivity and low-power consumption [7]. The use of micro-electromechanical systems (MEMS) is becoming increasingly popular for many applications, for example intra-cranial and intro-ocular pressure monitoring [8], [9]. This is largely due to the possibility of large scale manufacturing of devices with on-chip circuitry, which can improve effectiveness [10]. However, issues with packaging and reliability are still of concern [11]. Furthermore, the approach is only cost effective if production exceeds  $10^5$ – $10^6$  devices per year [12]. Alternatively, thick-film technology offers a reliable and repeatable method of producing pressure sensitive devices for use in medical applications. Furthermore, the process is extremely flexible, allowing a wide range of materials to be combined in order to produce a device with the required mechanical properties [13].

In this work, a prototype system based on capacitance-frequency-voltage conversion has been developed and used to evaluate the performance of thick-film interdigitated capacitors with different oxide-based dielectric layers. This system wirelessly transmits changes in capacitance with pressure to a receiver, which can operate at a range of 75 m in buildings and 300 m on open ground. Previous work, involving an interdigitated capacitor, using titanium dioxide ( $\text{TiO}_2$ ) as the dielectric layer, showed a high sensitivity to pressures in the range 0–17 kPa [14].

It is thought that the high response of the  $\text{TiO}_2$  devices can be attributed to the materials particle size. As a result, four oxides were investigated as part of this study, niobium pentoxide ( $\text{Nb}_2\text{O}_5$ ), cerium oxide ( $\text{CeO}_2$ ), magnesium oxide ( $\text{MgO}$ ), and  $\text{TiO}_2$ . These materials were also chosen on the basis of their relative biocompatibility and high bandgaps, making them ideal for the formation of a thick-film dielectric layer.  $\text{Nb}_2\text{O}_5$  is well known for its high corrosion resistance and thermodynamic stability. It often used in as an oxide coating for metallic implants and microoptical devices [15], [16]. In addition,  $\text{TiO}_2$  is commonly used for medical applications due to its cost effectiveness and chemical stability [17], [18].  $\text{MgO}$  is popular for use in electronic applications due to its wide bandgap [19]. Furthermore, nanoparticles of  $\text{MgO}$  have antiseptic properties due to

Manuscript received March 1, 2006; revised May 23, 2006; accepted June 6, 2006. This research was supported in part by the Enterprise Ireland Commercialization Fund 2003, as part of the MIAPS project, reference number CFTD/03/425, and in part by the Irish Research Council for Science, Engineering and Technology, funded by the National Development Plan. This is an expanded paper from the Sensors 2005 Conference. The associate editor coordinating the review of this paper and approving it for publication was Dr. Andre Bossche.

K. I. Arshak, O. Korostynska, and E. Jafer are with the Electronic and Computer Engineering Department, University of Limerick, Ireland (e-mail: khalil.arshak@ul.ie; olga.korostynska@ul.ie; essa.jafer@ul.ie).

D. Morris and A. Arshak are with the Physics Department, University of Limerick, Ireland (e-mail: deirdre.morris@ul.ie; arousian.arshak@ul.ie).

Color version of one or more of the figures in this paper is available at <http://ieeexplore.ieee.org>.

Digital Object Identifier 10.1109/JSEN.2006.886879

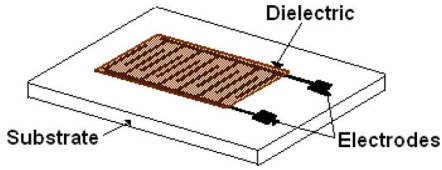


Fig. 1. Structure of a thick-film interdigitated capacitor.

their electric charge, which is opposite to that of bacteria [20]. Finally,  $\text{CeO}_2$  has a fluorite structure, which can deviate from stoichiometry as a function of temperature and/or pressure [21]. In addition, it is known that cerium which is introduced into the body orally is poorly absorbed by the digestive system and poses little risk to the individual [22].

In this study, the particle size of each oxide was examined using scanning electron microscopy (SEM). Their response to pressure, hysteresis and repeatability was evaluated using the wireless system. Finally the AC properties and the effect of temperature on each device were also recorded.

## II. EXPERIMENTAL PROCEDURE

The capacitors used in this study were fabricated by screen printing on Melinex substrates. The electrodes were formed using DuPont 4929 silver conductive paste and each had 25 fingers of length 6 mm and separation 0.2 mm. The sensor structure can be seen in Fig. 1. In each case, three layers of dielectric material were deposited over the electrodes, in order to prevent the formation of pinholes in the thick film. The baseline capacitances were measured to be 10.4, 7.3, 8.6, and 8 pF for  $\text{Nb}_2\text{O}_5$ ,  $\text{TiO}_2$ ,  $\text{CeO}_2$ , and  $\text{MgO}$ , respectively.

For parallel-plate or sandwich capacitors under pressure, the change in capacitance can be known by examining changes in the distance between the plates (or electrodes) in addition to the dielectric properties of the film between them [7]. The situation for interdigitated capacitors is more complex, with the capacitance being largely dependant on the number of fingers ( $N$ ), their length ( $L$ ), and width ( $W$ ), in addition to the gap between electrodes ( $G$ ), spatial wavelength ( $\lambda = 2(W + G)$ ), and the metallization ratio ( $\eta = 2W/\lambda$ ) [23]. It is found that, as all other parameters are fixed by the sensor design, it is the changing properties of the dielectric layer with pressure, which results in an alteration in capacitance [14], [23]–[25].

It can be seen that sandwich capacitors are largely dependant on the elastic properties of the electrodes. Their sensitivity to changes in pressure is due to a combination of geometrical and microstructural changes and can be varied by changing the distance between the electrodes. The contribution of the dielectric properties,  $\epsilon$ , cross-sectional area,  $A$ , and thickness of the dielectric layer,  $h$ , to the change in capacitance,  $C$ , can be seen in (1) [24]

$$\frac{dC}{C} = \frac{d\epsilon}{\epsilon} + \frac{dA}{A} - \frac{dh}{h}. \quad (1)$$

Unlike devices with a sandwich structures, the geometry of interdigitated electrodes is more fixed. Changes in capacitance with pressure are the result of the changing properties of the

dielectric layer,  $\epsilon$ , and changes in the electric field,  $E$ , near the electrodes, as shown in (2) [25]

$$\frac{dC}{C} = \frac{d\epsilon}{\epsilon} - \frac{dE}{E}. \quad (2)$$

To form the dielectric layer, each of the oxide powders was combined with 7 wt.% of binder, which in this case was polyvinyl butyral (PVB). A suitable amount of the solvent ethylenglycolmonobutylether was then added in order to make the paste, which was deposited onto the Ag electrodes by screen printing.

Once the capacitors were formed, SEM was performed using a Jeol JSM-840 in order to view the morphology and particle size of each oxide film. Their thickness was determined using a Sloan Dektak Profilometer. The response, hysteresis and repeatability of each device were evaluated using a specially designed, wireless, interface transmitter and receiver circuit. A thin waterproof flexible membrane of latex is used to protect each sensor from the liquid environment. During testing the change in capacitance for pressure ranging from 0–17 kPa was converted to a frequency change and wirelessly transmitted to an external receiver. The receiver then converts this frequency to a voltage, which is displayed as the output. This range was chosen after examining various pressures within the human body. For example, normal intra cranial pressure is approximately 1 kPa, while pressure in the gastrointestinal tract ranges from 6–16 kPa and arterial blood pressure is in the region of 13–18 kPa. In the future, work will be done to access the sensors performance under conditions, which mirror biological conditions.

## III. RESULTS AND DISCUSSION

### A. Interface, Transmitter and Receiver Circuit

To test the response of the thick-film pressure sensors an efficient wireless interface, transmitter, and receiver circuit was developed [26]. A block diagram of the system is shown in Fig. 2. The most important feature of the sensor interface circuit is an integrated capacitance to frequency converter. This connects the device to the telemetry subsystem. The sensor capacitance is first converted to a frequency using a low power TLC555 dual CMOS timer operating in an astable configuration. The output frequency can be approximated using (3)

$$f_{\text{out}} = \frac{1}{C_x(R_2 + 2R_1) \ln 2} \quad (3)$$

where,  $f_{\text{out}}$  is the output frequency,  $C_x$  is the sensor capacitance and the resistors  $R_1$ , and  $R_2$  are used to set up the timer frequency. In this case, they have the value  $R_1 = 100 \text{ k}\Omega$  and  $R_2 = 2 \text{ M}\Omega$ .

The frequency shift-keying (FSK) transmitter of 160 kbps has been selected to send the signal coming from the CMOS oscillator. The main advantage of using such a high-speed transmitter is that it can cope with large changes in capacitance during operation (3 to 55 pF). At the receiver side, a low power CD4046 phase-locked loop (PLL) integrated circuit is used as a frequency to voltage converter to display the output signal in terms of voltage levels. This is a micro-power device, typically

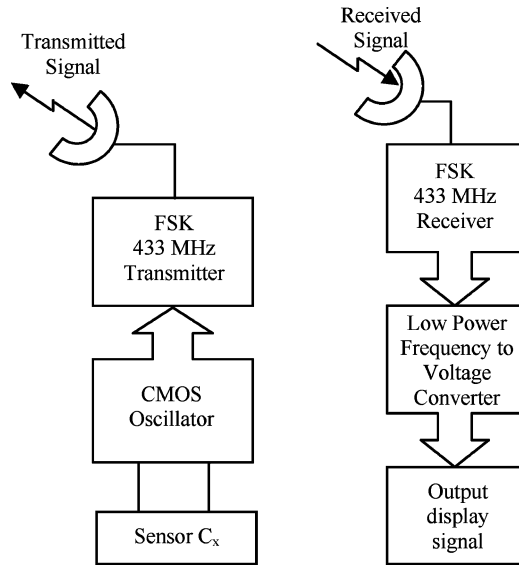


Fig. 2. Block diagram of the interface, transmitter, and receiver circuits.

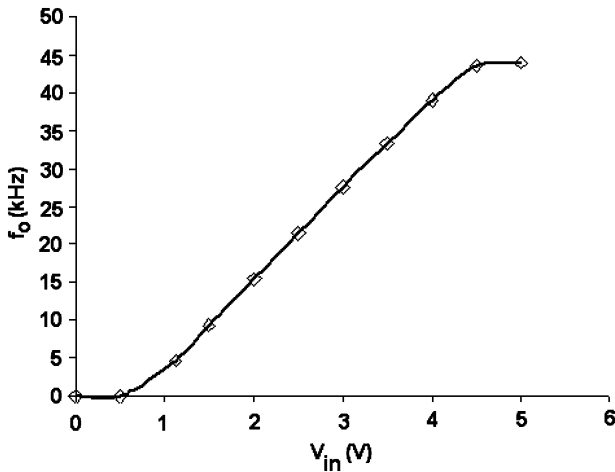


Fig. 3. Frequency/voltage characteristics of the voltage controlled oscillator.

drawing  $20 \mu\text{A}$ . The relationship between frequency  $f$  and voltage  $V$  can be seen in (4)

$$f = V \times 13.1 \text{ kHz} \quad (4)$$

where the value of  $13.1 \text{ kHz/V}$  is the slope of the graph showing the change in frequency with voltage for the voltage controlled oscillator (VCO). This is shown in Fig. 3.

### B. Morphology of the Oxide Thick Films

After printing, SEM was used to determine the morphology and particle size of each oxide, as this can have a large effect on the characteristics of each device. Previous examinations of the properties of nanocrystallite  $\text{TiO}_2$  have shown that it will exhibit plastic, rather than brittle behaviour. Furthermore, it was shown that the degree of ductility increases in response to decreasing grain sizes [27]. For example, the sensitivity of an interdigitated capacitor formed using  $\text{TiO}_2$  as the dielectric layer showed that

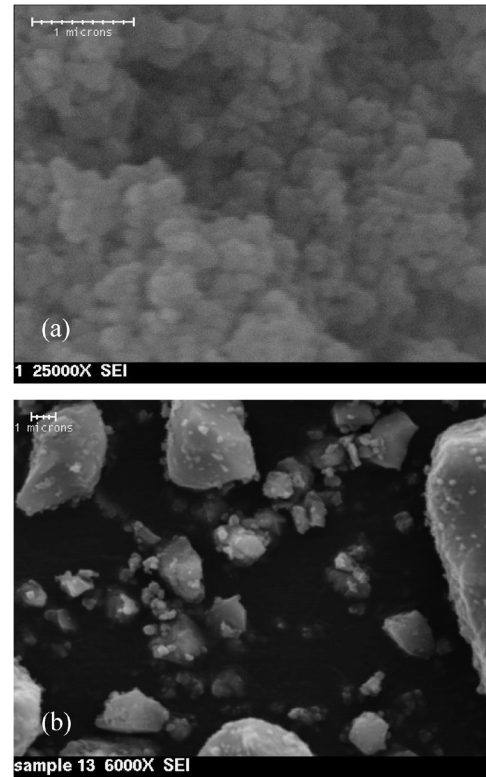


Fig. 4. SEM of  $\text{TiO}_2$  powder (a) prior to firing and (b) after firing.

the device has a high sensitivity to hydrostatic pressure with low hysteresis [14].

In this case, the  $\text{TiO}_2$  powder was mixed with isopropanol to form a slurry, which was wet ball milled in alcohol for 24 h [14]. The mixture was dried at  $120^\circ\text{C}$  to evaporate the alcohol. The powder was then placed under 2 tons of pressure to form a pellet, which was fired at  $1250^\circ\text{C}$  (at a rate of  $5^\circ\text{C}$  per minute) in a vacuum of  $6 \times 10^{-3}$  mbar for 5 h, followed by cooling (at a rate of  $3^\circ\text{C}$  per minute).

Firing the oxide powder before forming the paste can result in a change in the particle size and phase of the material. This can also be achieved by firing the thick-film layer after screen printing. However, if the film is to be fired after fabrication, the silver paste used for the electrodes cannot be polymer in nature. In addition, the ingredients for the thick-film paste must be changed to include a temporary binder, which is a polymer that is burnt off during firing, and permanent binder, which is a type of glass frit used to bind the oxide particles to each other and to the substrate. As a result, post firing of the oxide layer leads to a film, which is less compliant under an applied pressure [7].

The presence of  $\text{TiO}_2$  was confirmed by X-ray diffraction, while the change in materials particle size, caused by an alteration in phase, was determined by SEM, as shown in Fig. 4.

Using the system outlined in Section III-B, each sensor was tested under hydrostatic pressure by increasing the sensors depth in a liquid environment. This approach was chosen, since most biological environments are liquid in nature. As the pressure is increased, the sensors capacitance also increases due to deformation of the dielectric layer. This change is displayed

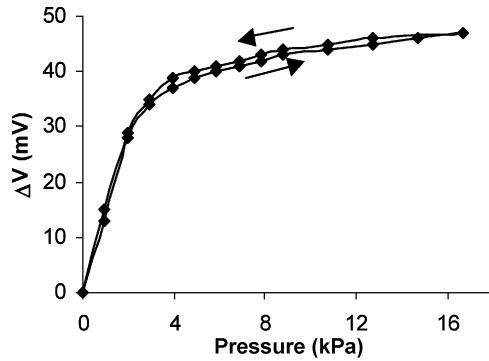


Fig. 5. Change in output voltage with pressure and hysteresis for prefired  $\text{TiO}_2$  device.

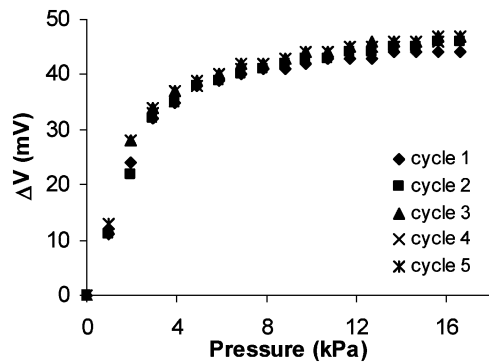


Fig. 6. Repeatability measured for prefired  $\text{TiO}_2$  sensors.

as a corresponding voltage at the receiver end of the circuit, as described by (3) and (4).

The sensitivity of each device was taken to be the maximum change in voltage over the entire pressure range. It was found to be 47 mV, as shown in Fig. 5, for the sensors investigated [14]. This corresponds to a change of approximately 2 pF, calculated using (3) and (4). It can be seen that the sensors response attenuates as the pressure increases. This can be partially attributed to the nonlinear characteristics of the PLL on the receiver side of the circuit.

Hysteresis was measured to be the maximum difference between loading and unloading cycles as a percentage of full-scale deviation. The hysteresis for the prefired  $\text{TiO}_2$  sample was calculated to be 4%, which corresponds to a voltage difference of 2 mV. This result can also be seen in Fig. 5.

In addition, the materials repeatability was measured by constant loading and unloading. The result over five cycles is shown in Fig. 6. The maximum difference between these was measured to be 4 mV, which is 8% when expressed as a percentage of full scale.

Fig. 7 shows SEM of each thick-film layer. It can be seen that the particle size of  $\text{Nb}_2\text{O}_5$  is in the range of 100–200 nm, while that of  $\text{TiO}_2$  also appears to be in the region of 200 nm. On the other hand, the  $\text{CeO}_2$  film appears to consist of flakes with particle sizes of approximately 5  $\mu\text{m}$  and the  $\text{MgO}$  film has particle sizes ranging from 0.5–5  $\mu\text{m}$ . It must also be observed that the  $\text{MgO}$  film is varied and uneven, while the  $\text{Nb}_2\text{O}_5$ ,  $\text{TiO}_2$  and  $\text{CeO}_2$  films are uniform in nature.

In addition to this measurement, the thickness of each layer after printing and drying was recorded using profilometry and found to be 70, 22.5, 36, and 66  $\mu\text{m}$  for  $\text{Nb}_2\text{O}_5$ ,  $\text{TiO}_2$ ,  $\text{CeO}_2$ , and  $\text{MgO}$ , respectively.

### C. Sensitivity of the $\text{Nb}_2\text{O}_5$ , $\text{TiO}_2$ , $\text{CeO}_2$ , and $\text{MgO}$ Capacitors

In this study, the oxides were not fired, prior to being formed into a paste and used to form capacitors. Each of the devices was tested as for the prefired  $\text{TiO}_2$  devices. The sensitivity of each device was determined by measuring their maximum response over the entire pressure range. Fig. 8 shows the response of each sensor.

It can be seen that the  $\text{Nb}_2\text{O}_5$  device is the most sensitive with a change in voltage of 65.9 mV over the entire range, followed by 45.5, 26.6, and 24.4 mV for  $\text{TiO}_2$ ,  $\text{MgO}$ , and  $\text{CeO}_2$ , respectively. This corresponds to a capacitance change of approximately 3, 1.9, 1.2, and 1 pF, respectively, using (1) and (2). It should also be observed that the decrease in sensitivity corresponds to the increase in each materials particle size. The inflection point, which occurs at approximately 4 kPa, is most likely due to the presence of the polymer layer, which protects the device from the liquid environment. It may be overcome by changing the method by which the sensor is coated in addition to altering the interface circuit so that the capacitance could be read directly, without the influence of the PLL.

Hysteresis is caused by friction and structural changes within the material and can lead to inaccuracies in the recorded pressure [28]. High levels of hysteresis in thick-film devices can also be attributed to the method of paste preparation, the presence of large particles, greater than 2  $\mu\text{m}$ , within the printed film and differences in the temperature coefficient of expansion (TCE) of the substrate and the thick films [29]. In this work, the hysteresis of each device was recorded for consecutive loading and unloading, by expressing the difference between cycles as a percentage of full scale. It was found that  $\text{Nb}_2\text{O}_5$  displayed the largest changes between loading and unloading, as shown in Fig. 9. The hysteresis recorded was 7.7%, 3.8%, 7.4%, and 6.8% for  $\text{Nb}_2\text{O}_5$ ,  $\text{TiO}_2$ ,  $\text{CeO}_2$ , and  $\text{MgO}$ , respectively.

These values correspond with those recorded for other thick-film devices using capacitor configurations (5%–30%) [31]. More particularly, the hysteresis recorded for unfired  $\text{TiO}_2$  devices corresponds with that previously recorded for the fired interdigitated capacitors, and, in addition, there is little difference in sensitivity.

It is important to note that the high sensitivity displayed by the  $\text{Nb}_2\text{O}_5$  devices is accompanied by a large value for the hysteresis. Such behaviour has previously been observed for a polymer thick-film device [31]. However, previous investigations into the response of  $\text{V}_2\text{O}_5$  strain gauges showed that a variance due to the variable valency of the vanadium ion could be overcome by the addition of a second oxide [32]–[34].

To assess the long-term stability of each device, they were placed under a constant pressure of 7 kPa for a 24-h period. The results are shown in Fig. 10. It is expected that some changes should occur due to the viscoelastic behaviour of the polymer component in the oxide thick film [34].

It was found that for  $\text{TiO}_2$ ,  $\text{CeO}_2$ , and  $\text{MgO}$ , the change in capacitance with time was less than 5%. The capacitance of

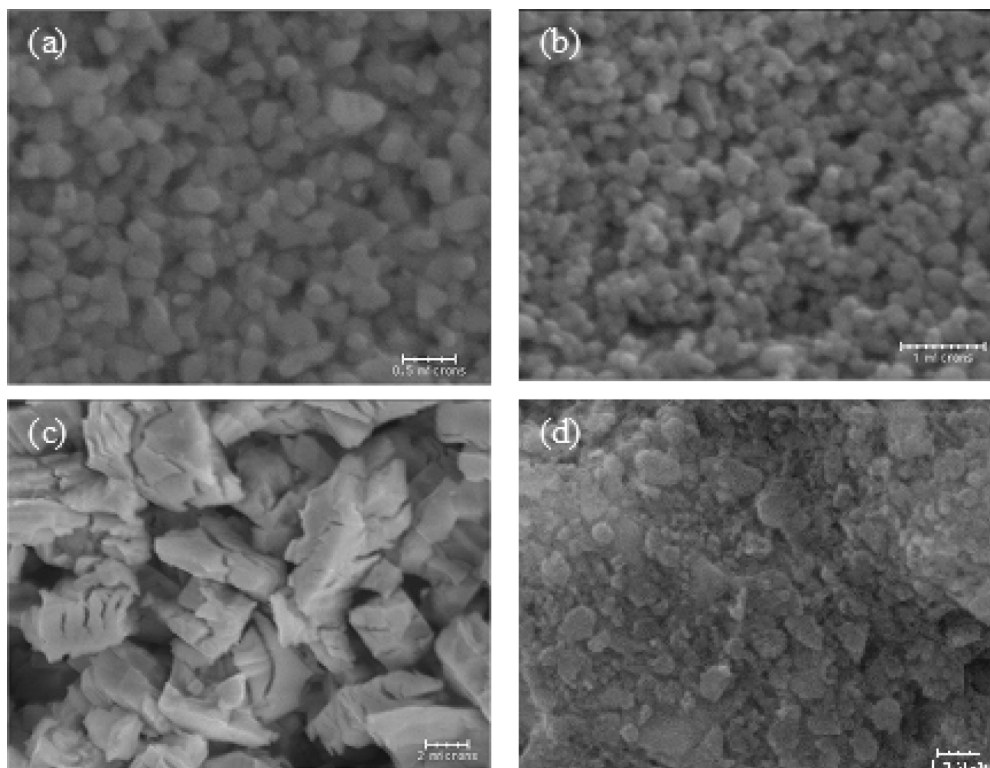


Fig. 7. SEM of (a)  $\text{Nb}_2\text{O}_5$ , (b)  $\text{TiO}_2$  (c)  $\text{CeO}_2$ , and (d)  $\text{MgO}$  thick films.

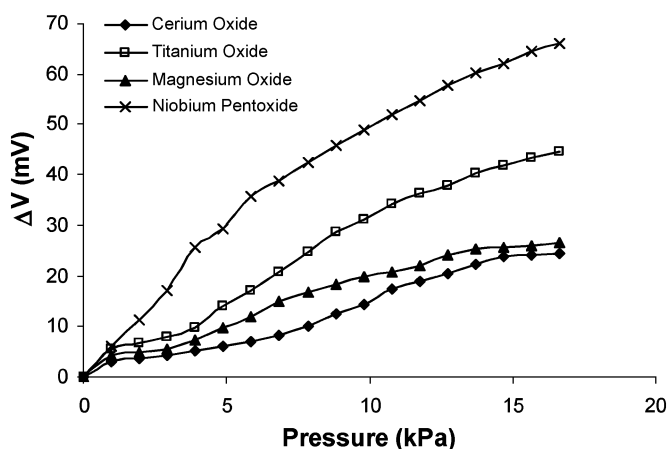


Fig. 8. Change in output voltage with pressure for each of the oxides under investigation.

the  $\text{MgO}$  sample fluctuated between increasing and then decreasing with time. This may be due to the uneven nature of the thick-film, as can be seen in Fig. 2. In addition, the  $\text{Nb}_2\text{O}_5$  interdigitated capacitor was extremely unstable, with the capacitance dropping by 10 pF in the first 2 h. It is thought that the stability of this material could be further improved by mixing it with another oxide, as discussed previously. However, as in the case of a  $\text{V}_2\text{O}_5$ - $\text{CeO}_2$  thin-film strain gauge, the addition of a second phase may affect the sensitivity [34].

Oxide materials are popular for use both thin- and thick-film strain gauges and pressure sensors due to their strong piezoresistive properties. In terms of their sensitivity, thin-film strain gauges have the potential to possess a higher gauge factor, or

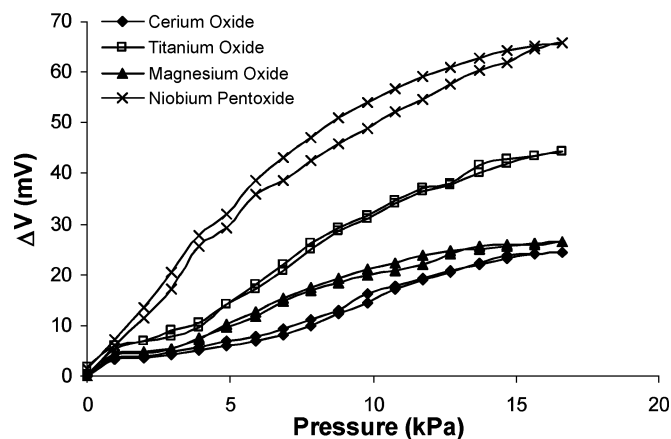


Fig. 9. Hysteresis measured for  $\text{Nb}_2\text{O}_5$ ,  $\text{TiO}_2$ ,  $\text{CeO}_2$ , and  $\text{MgO}$  interdigitated capacitors.

sensitivity, than their thick-film counterparts [36]. However, thick-film technology allows a wider combination of materials and conductive fillers to be used and have successfully been combined to produce a device with a gauge factor as high as 80 [31]. Optimized thin-film devices based on  $\text{V}_2\text{O}_5$ ,  $\text{Bi}_2\text{O}_3$  had a gauge factor of 16 [33].

#### IV. AC PROPERTIES

In order to develop suitable interface circuitry for a thick-film capacitor, knowledge of the frequency dependence of the materials properties is required. With this in mind, the change in capacitance with frequency for each device was examined using

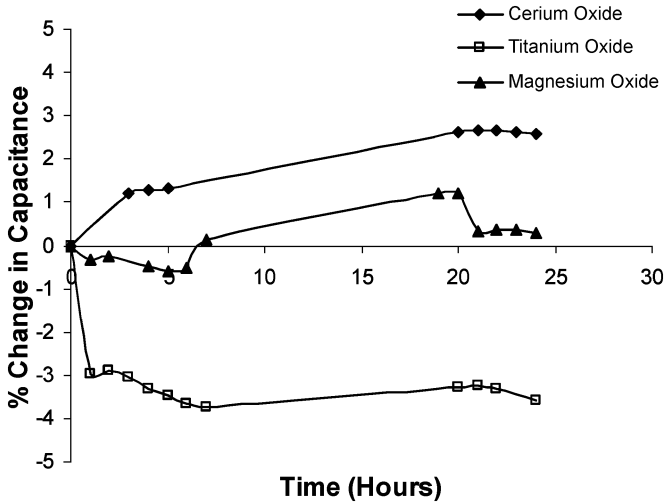


Fig. 10. Change in capacitance with time for  $\text{TiO}_2$ ,  $\text{CeO}_2$ , and  $\text{MgO}$  interdigitated capacitors.

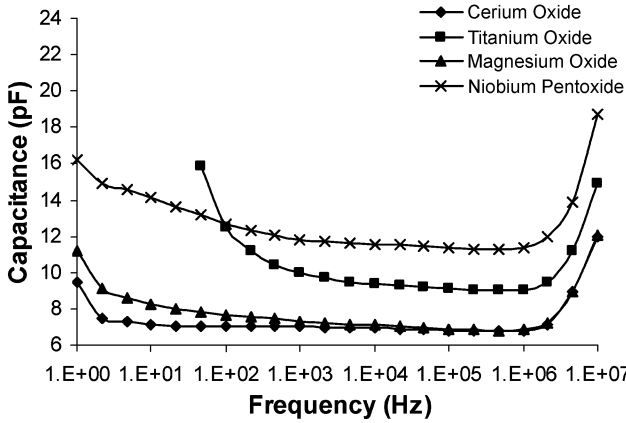


Fig. 11. Change in capacitance with frequency for  $\text{Nb}_2\text{O}_5$ ,  $\text{TiO}_2$ ,  $\text{CeO}_2$ , and  $\text{MgO}$  interdigitated capacitors.

a Solartron S1 1260 Impedance/Gain Phase Analyser and associated software which measures and records the sensor capacitance for frequencies in the range 1 Hz to 10 MHz.

Previous work, which details the development of a thick-film sandwich capacitor for strain sensing applications, has shown that device sensitivity is affected by operating frequency [37]. The differences have been attributed to changes in dissipation factor, which is a measure of how capacitive the thick-film device is. It can be seen from Fig. 11 that each device is stable in the range 1 kHz–1 MHz. However, there is considerable variation in the values of capacitance outside this range, especially in the case of  $\text{TiO}_2$ , where the capacitance increases sharply for frequencies below 1 kHz. This data is not shown in Fig. 11 for clarity. Therefore, some difference in the device sensitivity may be expected for changes in the operating frequency.

## V. TEMPERATURE EFFECTS

One of the major concerns with thick-film devices is the high-temperature dependence of capacitors that operate by measuring the change in distance between two electrodes, one of which is free to move, while the other is stationary [38]. While there

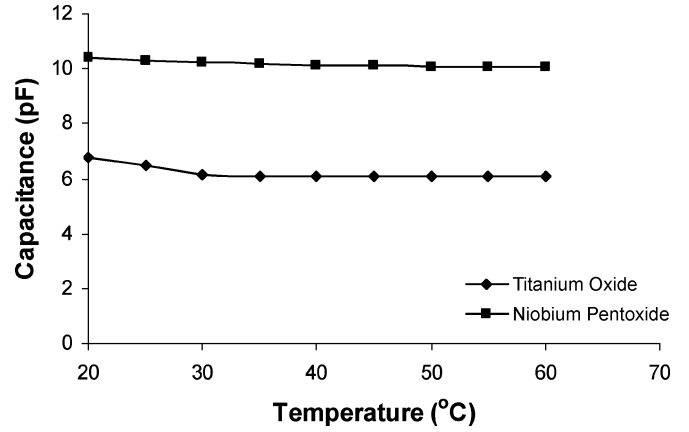


Fig. 12. Change in capacitance with temperatures in the range  $20\text{ }^\circ\text{C}$ – $60\text{ }^\circ\text{C}$  for  $\text{Nb}_2\text{O}_5$  and  $\text{TiO}_2$  devices.

are no moving parts in interdigitated capacitors, it is still necessary to account for any alteration in capacitance, which may occur due to temperature changes. Therefore,  $\text{Nb}_2\text{O}_5$  and  $\text{TiO}_2$  devices were tested in the temperature range  $10\text{ }^\circ\text{C}$ – $60\text{ }^\circ\text{C}$ , as these were the most sensitive to changes in hydrostatic pressure. The temperature coefficient of capacitance (TCC), which is the parts per million change in capacitance per degree change in temperature, was calculated using (5)

$$\text{TCC} = \frac{C_{t_2} - C_{t_1}}{C_{t_1} \Delta T} 10^6 \quad (5)$$

where  $C_{t_1}$  is the capacitance at temperature 1,  $C_{t_2}$  is the capacitance at temperature 2, and  $\Delta T$  is the change in temperature. In this work, the TCC was calculated over two temperature regions. Region 1 extends from  $10\text{ }^\circ\text{C}$  to  $20\text{ }^\circ\text{C}$  and region 2 covers the temperatures  $20\text{ }^\circ\text{C}$ – $60\text{ }^\circ\text{C}$ .

The TCC for region 1 was  $1981\text{ ppm}/^\circ\text{C}$  and  $99902\text{ ppm}/^\circ\text{C}$  for  $\text{Nb}_2\text{O}_5$  and  $\text{TiO}_2$ , respectively. This shows that there is a high sensitivity to changes below room temperature, in the case of the  $\text{TiO}_2$  devices. It can be seen from Fig. 12 that both devices are extremely stable over the temperature range of region 2. The TCC was calculated to be  $770\text{ ppm}/^\circ\text{C}$  and  $2680\text{ ppm}/^\circ\text{C}$ , respectively. Typical values expected for thick-film capacitors are  $1500$ – $3000\text{ ppm}/^\circ\text{C}$ . So, it can be seen that the values for  $\text{Nb}_2\text{O}_5$  are well within or better than normal for each temperature range, while  $\text{TiO}_2$  is only suitable for use at temperatures greater than  $20\text{ }^\circ\text{C}$ . This will affect its potential use in situations where the temperature cannot be controlled. However, both devices are suitable for use in biomedical applications.

## VI. CONCLUSION

In this work, the sensitivity of four oxide materials was evaluated using a wireless pressure measurement system, which was designed in house. Each oxide was screen printed onto interdigitated electrodes and tested in the range  $0$ – $17\text{ kPa}$ . The system successfully transmitted information on the voltage changes, related to the sensor capacitance, with pressure. It was found that  $\text{Nb}_2\text{O}_5$  devices were most sensitive, followed by  $\text{TiO}_2$ ,  $\text{MgO}$ , and  $\text{CeO}_2$ . The range of response may in part be

due to the different particle sizes as nanosized TiO<sub>2</sub> particles have been shown to exhibit more ductile behaviour and, therefore, are more easily deformed under pressure. The response of Nb<sub>2</sub>O<sub>5</sub> and TiO<sub>2</sub> devices to temperature changes has also been evaluated. It is found that both are stable at temperatures greater than 20 °C. However, TiO<sub>2</sub> is not suited for use below this value. It is concluded that all the materials investigated as part of this work displayed a high sensitivity to pressure changes with the materials which possess the smallest particle size displaying the largest responses. These devices are suitable candidates for use in a wireless pressure monitoring system.

## REFERENCES

- [1] C. May, T. Finch, F. Mair, and M. Mort, "Towards a wireless patient: Chronic illness, scarce care and technological innovation in the United Kingdom," *Social Sci. Med.*, vol. 61, pp. 1485–1494, 2005.
- [2] C. Yang, C. Zhao, L. Wold, and K. R. Kaufman, "Biocompatibility of a physiological pressure sensor," *Biosens. Bioelectron.*, vol. 19, pp. 51–58, 2003.
- [3] G. Schimetta, F. Dollinger, G. Scholl, and R. Weigel, "Optimized design and fabrication of a wireless pressure and temperature sensor unit based on SAW transponder technology," presented at the IEEE Int. Symp. Dig. MTT-S, Denver, CO, 2001, unpublished.
- [4] T. Umeno, K. Asano, H. Ohashi, M. Yonetani, T. Naitou, and T. Taguchi, "Observer based estimation of parameter variations and its application to tyre pressure diagnosis," *Control Eng. Practice*, vol. 9, pp. 639–645, 2001.
- [5] M. Zagnoni, A. Golfarelli, S. Callegari, A. Talamelli, V. Bonora, E. Sangiorgi, and M. Tartagni, "A non-invasive capacitive sensor strip for aerodynamic pressure measurement," *Sens. Actuators A*, to be published.
- [6] T. Grandke and W. H. Ko, *Sensors: A Comprehensive Survey*. New York: VCH, 1989, vol. 1.
- [7] R. Puers, "Capacitive sensors: When and how to use them," *Sens. Actuators A*, vol. 37–38, pp. 93–105, 1993.
- [8] B. B. Flick and R. Orglmeister, "A portable microsystem-based telemetric pressure and temperature measurement unit," *IEEE Trans. Biomed. Eng.*, vol. 47, pp. 12–16, 2000.
- [9] P.-J. Chen, D. C. Rodger, M. S. Humayun, and Y.-C. Tai, "Unpowered spiral-tube parylene pressure sensor for intraocular pressure sensing," *Sens. Actuators A*, to be published.
- [10] T. Akin, "Silicon micromachining and microfabrication techniques for integrated sensor and actuator systems," in *Proc. IEEE Mediterranean Electrotechnical Conf.*, Antalya, Turkey, 1994, pp. 529–532.
- [11] A. Arshak, K. Arshak, D. Waldron, D. Morris, O. Korostynska, E. Jafer, and G. Lyons, "Review of the potential of a wireless MEMS and TFT microsystem for the measurement of pressure in the GI tract," *Med. Eng. Phys.*, vol. 27, p. 347, 2005.
- [12] D. Crescini, V. Ferrari, D. Marioli, and A. Taroni, "A thick-film capacitive pressure sensor with improved linearity due to electrode shaping and frequency conversion," *Meas. Sci. Technol.*, vol. 8, pp. 71–77, 1997.
- [13] M. R. Neuman, R. P. Buck, V. V. Cosofret, E. Linder, and C. C. Liu, "Fabricating biomedical sensors with thin-film technology," *IEEE Eng. Med. Biol. Mag.*, vol. 13, pp. 409–419, 1994.
- [14] K. Arshak, A. Arshak, D. Morris, O. Korostynska, and E. Jafer, "A wireless pressure measurement system based on TiO<sub>2</sub> interdigitated electrodes," presented at the IEEE Sensors Conf., Irvine, CA, unpublished.
- [15] F. Richter, H. Kupfer, P. Schlott, T. Gessner, and C. Kaufmann, "Optical properties and mechanical stress in SiO<sub>2</sub>/Nb<sub>2</sub>O<sub>5</sub> multilayers," *Thin Solid Films*, vol. 389, pp. 278–283, 2001.
- [16] D. Velten, E. Eisenbarth, N. Schanne, and J. Breme, "Biocompatible Nb<sub>2</sub>O<sub>5</sub> thin films prepared by means of the sol-gel process," *J. Mater. Sci.*, vol. 15, pp. 457–461, 2004.
- [17] D. M. Brunette, *Titanium in Medicine: Material Science, Surface Science, Engineering, Biological Responses and Medical Applications*. London, U.K.: Springer, 2001.
- [18] H. Liu and L. Gao, "Synthesis and properties of CdSe-sensitized rutile TiO<sub>2</sub> nanocrystals as a visible light-responsive photocatalyst," *J. Amer. Ceram. Soc.*, vol. 88, p. 1020, 2005.
- [19] S. Schintke, S. Messerli, M. Pivetta, F. Patthey, L. Libiouille, M. Stengel, A. De Vita, and W.-D. Schneider, "Insulator at the ultrathin limit: MgO on Ag(001)," *Phys. Rev. Lett.*, vol. 87, pp. 276081–276084, 2001.
- [20] N. G. Ma, J. Lang, and D. H. L. Ng, "Preparation of MgO and Fe nanostructure in Mg matrix composite by reaction sintering," *Composites Sci. Technol.*, vol. 65, pp. 2167–2173, 2005.
- [21] K. Arshak and O. Korostynska, "λ-Radiation sensing properties of cerium oxide based thick film structures," *Sens. Actuators A*, vol. 115, pp. 196–201, 2004.
- [22] J. Gomez-Aracena, R. A. Riemersma, M. Gutierrez-Bedmar, P. Bode, J. D. Kark, A. Garcia-Rodriguez, L. Gorgojo, P. van't Veer, J. Fernandez-Crehuet, F. J. Kok, and J. M. Martin-Moreno, "Toenail cerium levels and risk of a first acute myocardial infarction: The EURAMIC and heavy metals study," *Chemosphere*, to be published.
- [23] R. Igreja and C. J. Dias, "Analytical evaluation of the interdigital electrodes capacitance for a multi-layered structure," *Sens. Actuators A*, vol. 112, pp. 291–301, 2004.
- [24] A. Arshak, K. Arshak, D. Morris, O. Korostynska, and E. Jafer, "Investigation of TiO<sub>2</sub> thick film capacitors for use as strain gauge sensors," *Sens. Actuators A*, vol. 122, pp. 242–249, 2005.
- [25] T. R. Filanc-Bowen, G. H. Kim, and Y. M. Shkel, "Novel sensor technology for shear and normal strain detection with generalized electrostriction," in *Proc. IEEE Sensors Conf.*, 2002, vol. 2, pp. 1648–1652.
- [26] K. Arshak, E. Jafer, J. Orr, A. Arshak, D. Morris, O. Korostynska, D. McDonagh, J. D. Quartararo, H. Dampfling, and C. Y. Huang, "Design of a low power capacitive pressure sensor signal-conditioning interface using PLL," presented at the 3rd Int. Conf. Systems Signals and Devices, Sousse, Tunisia, 2005.
- [27] B. Jiang and G. J. Weng, "A theory of compressive yield strength of nano-grained ceramics," *Int. J. Plastic.*, vol. 20, pp. 2007–2026, 2004.
- [28] *Handbook of Modern Sensors: Physics, Designs, and Applications*. New York: Springer-Verlag, 1996.
- [29] K. Arshak, F. Ansari, D. McDonagh, and D. Collins, "Development of a novel thick-film strain gauge sensor system," *Meas. Sci. Technol.*, vol. 8, pp. 58–70, 1997.
- [30] A. Arshak, K. I. Arshak, D. Morris, O. Korostynska, and E. Jafer, "Development of PVDF thick film interdigitated capacitors for pressure measurement on flexible melinex substrates," presented at the MRS Spring Meeting, San Francisco, CA, 2005, unpublished.
- [31] K. I. Arshak, A. K. Ray, C. A. Hogarth, D. G. Collins, and F. Ansari, "An analysis of polymeric thick-film resistors as pressure sensors," *Sens. Actuators A*, vol. 49, pp. 41–45, 1995.
- [32] K. Arshak and R. Perrem, "Fabrication of a thin-film strain-gauge transducer using Bi<sub>2</sub>O<sub>3</sub>-V<sub>2</sub>O<sub>5</sub>," *Sens. Actuators A*, vol. 36, pp. 73–76, 1993.
- [33] K. I. Arshak, G. A. Landers, and R. L. Perrem, "Investigation into the properties of the mixed oxide V<sub>2</sub>O<sub>5</sub>-CeO<sub>2</sub> for use as a thin film strain gauge sensor," *Int. J. Electron.*, vol. 76, pp. 1011–1022, 1994.
- [34] K. I. Arshak and R. L. Perrem, "The correlation of the electrical and optical properties of thin films of V<sub>2</sub>O<sub>5</sub>-Bi<sub>2</sub>O<sub>3</sub>," *J. Phys. D*, vol. 26, pp. 1098–1102, 1993.
- [35] T. A. Osswald and G. Menges, *Materials Science of Polymers for Engineers*, 2nd ed. Munchen, Germany: Carl Hanser Verlag, 2003.
- [36] K. Arshak, D. Morris, A. Arshak, and O. Korostynska, "Development of high sensitivity oxide based strain gauges and pressure sensors," *J. Mater. Sci.*, to be published.
- [37] K. I. Arshak, D. McDonagh, and M. A. Durcan, "Development of new capacitive strain sensors based on thick film polymer and cermet technologies," *Sens. Actuators A*, vol. 79, pp. 102–114, 2000.
- [38] P. G. Dargie and S. T. Hughes, "A thick-film capacitive differential pressure transducer," *Meas. Sci. Technol.*, vol. 5, pp. 1216–1220, 1994.



**Khalil I. Arshak** (M'95) received the M.Sc.

degree from Salford University, U.K., in 1979, and the Ph.D. and D.Sc. degrees from Brunel University, U.K., in 1986 and 1998, respectively.

He joined the University of Limerick, Limerick, Ireland, in 1986, where he leads the Microelectronic and Semiconductor Research Group. He has authored more than 240 research papers in the area of microelectronics and thin- and thick-film technology. His current research interests include

lithography process modeling, TSI processes characterization, mixed-oxide thin- and thick-film sensor development, and application specific integrated circuit design.



**Deirdre Morris** received the B.Sc. degree in applied physics from the University of Limerick, Limerick, Ireland, in 2003. She is currently pursuing a higher degree by research.

Her areas of interest include thick-film devices for use as pressure sensors and strain gauges.



**Olga Korostynska** received the B.Sc. and M.Sc. degrees in biomedical electronics from the National Technical University of Ukraine (KPI), Kyiv, in 1998 and 2000, respectively, and the Ph.D. degree from the University of Limerick, Limerick, Ireland, in 2003.

Her research interests are in thin- and thick-film technologies, material properties characterization, and thin-/thick-film sensors.



**Arousian Arshak** received the M.Sc. degree

from Salford University, U.K., in 1979, and the Ph.D. degree from the University of Limerick (UL), Limerick, Ireland, in 1990.

She is currently a Lecturer in the Department of Physics, UL, where she specializes in the areas of photolithography, silylation (gas phase), and plasma etching. Other areas of interest include radiation damage in thin and thick films, the microstructure of electrodeposited copper, and thin- and thick-film

sensors.



**Essa Jafer** received the B.Sc. and M.Sc. degrees in 1994 and 1999, respectively, in electronic and communications engineering from the University of Baghdad, Baghdad, Iraq, and the M.Eng. (research) degree in 2003 from the Electronic and Computer Engineering (ECE) Department, University of Limerick, Limerick, Ireland.